



Two- and three dimensional analysis on brain oxygen delivery.

Quistorff, Bjørn; Chance, Britton

Published in:
Oxygen and Physiological Function

Publication date:
1976

Document version
Publisher's PDF, also known as Version of record

Citation for published version (APA):
Quistorff, B., & Chance, B. (1976). Two- and three dimensional analysis on brain oxygen delivery. *Oxygen and Physiological Function*, 100-110.

**TWO - AND THREE DIMENSIONAL
ANALYSIS ON BRAIN OXYGEN DELIVERY**

B. Quistorff, B. Chance

**The Johnson Research Foundation, Department of Biophysics and Biochemistry,
University of Pennsylvania, Philadelphia, Pennsylvania**

Reprinted with permission from
**OXYGEN AND PHYSIOLOGICAL
FUNCTION**

Edited by

Frans F. Jöbsis

© 1976 by Professional Information Library
1616 Hi-Line Drive, Dallas, Texas

TWO- AND THREE-DIMENSIONAL ANALYSIS ON BRAIN OXYGEN DELIVERY

B. Quistorff, B. Chance
The Johnson Research Foundation
Department of Biophysics and Biochemistry
University of Pennsylvania
Philadelphia, Pennsylvania

Looking through the optical microscope at mammalian tissues such as heart, brain or liver, it is largely composed of mitochondria. Particular cardiac tissues where 34% of the tissue volume is occupied by mitochondria. The vital function of the mitochondria is to convert energy liberated from substrate oxidation to synthesis of ATP. This process locates almost all the oxygen consumption of the cell to the mitochondrial compartment. So, aiming at a mapping of the oxygen delivery pattern in a tissue, it would seem logical to measure a parameter inside the mitochondria, which indicates the balance between oxygen availability and the actual oxygen consumption. NADH is in fact such an endogenous probe of the redox state and it is highly sensitive to oxygen tension (3). NADH is easy to measure as it has a strong and specific fluorescence signal - it can even be measured just by taking a photograph with the appropriate filters for excitation and emission light (9). However, if only the NADH signal is measured, regions with low mitochondrial concentration would appear less reduced than regions with more mitochondria even though both had the same redox state. Furthermore, it is known that the presence of hemoglobin interferes with PN fluorescence. To overcome such distribution and screening problems one would like to measure two components from the respiratory chain - one which indicates the degree of oxidation and the other indicating the degree of reduction, e.g., the redox ratio.

THE FP/PN RATIO TECHNIQUE

Figure 1 shows the sequence of the respiratory carriers from NADH to oxygen. Of these, flavoprotein is fluorescent in the oxidized form. Especially FP_L , identified with lipoate dehydrogenase, has a strong fluorescence signal (2). Pyridine nucleotide (PN) and flavoprotein (FP) are in rapid equilibrium at almost the same potential (2), so measuring these two components and calculating the ratio between them would provide a sensitive measure of the redox state of the respiratory chain; i.e. a high FP/PN ratio will indicate an oxidized level - a low ratio a reduced level. As mentioned above one would expect the FP/PN ratio to be insensitive to changes in mitochondrial - and hemoglobin concentration. Figure 2 confirms that. A variation in mitochondrial concentration from 1 - 10 mg mitochondrial protein per ml does not affect the ratio as flavoprotein and pyridine nucleotide fluorescence are nearly equally decreased (Fig. 2A). The same result is seen in Fig. 2B where variation in hemoglobin concentra-

tions were simulated. Fluorescence intensity is generally increased at low temperatures. It has been shown recently (7) that the NADH emission peak at 450 nm after 366 nm excitation is much sharper and about 10 fold more intense at 77°K as compared with room temperature measurements. Also the flavoprotein signal is substantially increased at low temperature. So we conclude that the two problems of distribution and screening errors in scanning for the tissue redox state, are largely eliminated by using the ratio technique, and by the use of low temperatures.

Our approach to the three dimensional mapping of the redox-state of the brain In Vivo involve the following steps: 1) Freeze clamping of the brain; 2) cutting and milling of the frozen sample; 3) 2-dimensional low temperature redox ratio scanning; and 4) display of the data.

TISSUE SAMPLING

The ideal tissue sampling procedure must fulfill three requirements: 1) Preservation of In Vivo metabolic characteristics of the tissue; 2) preservation of tissue morphology and/or sampling with known morphological origin; and 3) sampling with the animal in a series of different physiological conditions must be possible. The Guillotine-freeze clamping technique, described in detail elsewhere (13) is especially suited to whole animal organ study and will meet the above requirements for rat brain sampling as described below. Sampling from anaesthetized as well as from unanaesthetized rats can be performed. The un-anaesthetized rat is restrained in a transparent tube in the sampling instrument as shown in Fig. 3 and schematically in Fig. 4. The position in the tube provides for easy change and control of the physiological condition of the animal; i.e., the gas mixture inhaled can be changed in less than a second and blood gas tensions, pH and blood pressure monitored via a tail-artery catheter (10). The brain sampling is performed by means of two rotating knives which cuts out a cross section of the head of the animal (Fig. 4A). The slice contains the desired part of the brain and is immediately freeze clamped between two aluminum blocks precooled in liquid nitrogen (Fig. 4B). The total sampling procedure works automatically and lasts about a tenth of a second. The position of the rat in the tube is adjusted by means of a constriction and a stopper, so that the knife corresponding to the left of the two vertical dotted lines on Fig. 4A will pass through the part of the brain to be examined; the other will decapitate the animal. The tip of the nose of the rat is used as a landmark in this adjustment procedure and experience shows that any region of the brain may be sampled within an accuracy of ± 1 mm. The thickness of the slice cut out is 13 mm, but can be varied between 4 and 15 mm. However, the thinner the cut the more distortion of the gross morphology in the slice. The freeze clamping tongs are adjusted to compress the 13 mm head slice to a final thickness of 9 - 10 mm. This is not a very efficient freeze clamping in as much as only a smaller part of the sample (see later) is frozen sufficiently rapid to freeze stop the metabolic state at the In Vivo level. On the other hand the "gentle" freeze clamping accomplished by compressed air operated cooling tongs preserves the morphology in the frozen sample very well, Fig. 9A.

TISSUE CUTTING AND GRINDING

In order to measure the redox state in three dimensions a technique for cutting of the brain sample must be applied. Any heating of the tissue above a temperature of -50°C even for a short period of time will change

the redox state towards more reduced level (4). A special tissue miller operated at 77⁰K was constructed (12). Figure 5 shows the instrument on a simplified diagram. A cutter wheel is mounted under liquid nitrogen and is driven via a chain, at a speed of 1000 rpm. The sample is clamped in a holder connected to a micrometer screw by which the sample is moved against the cutter. The smallest possible increment with this instrument is 30 μ . The surface of the sample is milled as the sample holder is projected against the rotating cutter wheel.

THE SCANNER

After the grinding the sample is transferred to the redox ratio scanner which is shown schematically in Fig. 6. The fluorometer unit is based upon earlier design of four-channel time-sharing fluorometer, for a comparison see Chance, et al (5). Pyridine nucleotide was excited at 366 \pm 30 nm and emission was read at 450 \pm 30 nm. Excitation of flavoprotein was performed in a rather narrow region around 463 \pm 10 nm to avoid the interference due to changes in cytochrome absorption. The flavin emission was read at 540 \pm 20 nm, even though the emission spectrum (7) shows that fluorescence is in fact peaking at 520 nm, because filters including this region with sufficient cut off against the 463 excitation were not available at that time. The excitation source is a 100 W Mercury arc for 366 nm and a 45 W tungsten lamp for 463 nm, both water cooled. The beams are brought together via a dichroic mirror (95% reflectance below 370 nm). The optical coupling from the fluorometer to the sample is performed via two light guides merged on the sample surface in a concentric configuration (see Fig. 6) (14). All seven fibers are 80 μ glass covered UV transmittent glass fibers. The central one, connected to the PMT, reads the fluorescence signal, whereas the six surrounding fibers transmit the excitation to the tissue surface. The optimal distance between the light guide and the surface has been found to 175 - 225 μ . At this distance the resolution is about 150 μ . The sample is partially submerged under liquid nitrogen in a Styrofoam Dewar. The tip of the light guide is connected to stepper motor operated precision crossways which moves it horizontally parallel to the tissue surface with a minimum step size of 15 μ . As mentioned the tip of the light guide is also moveable in the Z-axis, by means of a manually operated micrometer screw. To prevent moisture condensation on the sample surface and on tip of the light guide during scanning, there is a lid on the styrofoam Dewar, equipped with an aperture, which can be narrowed to allow only the scanning movements of the light guide. Furthermore, there is a constant passage of cold, dry nitrogen (the gas phase from the liquid nitrogen storage tank) to the inside of the Dewar, while warm, dry nitrogen is blown over the opening of the lid (See Fig. 6). The level of liquid nitrogen can easily be controlled in the right-hand part of the u-shaped Dewar.

DATA READING IN TWO- AND THREE-DIMENSIONS

The read out of the flavoprotein and pyridine nucleotide signals and the x-y scanning movements are computer directed. The scanning is stepwise and proceeds as shown in Fig. 8. The light guide is manually operated to the starting position on the sample surface, so that the area of special interest is located in the first quadrant of the scanning coordinate system. The x and y scanning distances and the step size desired for the actual scan are chosen. (See Fig. 8). Five individual readings are made of flavoprotein and pyridine nucleotide fluorescence in each point. The average FP and PN values are then stored in the computer - the first point with the

coordinates 1, 1., the second with the coordinates, 1,2, etc. The two dimensional scan is completed when all points within the predetermined area have been read. Repeating the 2-D scan after milling of the sample surface provide for 3-D data collection.

DISPLAY OF DATA

The data from each 2-D scan are basically available as the raw analog data, for example, in the form of a matrix where the numbers give the intensity of one of the parameters (FP,PN or FP/PN) in every coordinate point. The matrix can easily be converted to a contour plot by drawing the "iso-intensity lines": (11) or, if the individual numbers in the matrix are translated to a gray scale, it can be displayed, for example on a TV monitor giving the FP, PN or redox ratio image where the most oxidized points on the sample surface show up white and the reduced black. Figure 8A shows a reconstructed 2-D PN-image of a test pattern together with the photographic image (Fig. 8B). The test pattern is a pencil drawing on white paper which has a strong fluorescence at 450 nm. Therefore the "PN signal" from the pencil lines will appear dark on the reconstructed image. The scanning was performed with a step size of 0.1 mm over a 3 by 3 mm area. To provide for a qualitative comparison of the two image forming techniques, the photographic picture was enlarged correspondingly to 10 linepairs per mm.

A display of the three dimensional data is obtained by combining the relevant data from consecutive 2-D scans. There are however, two limitations to consider for the 3-D mapping. One is the depth of origin of the fluorescence in the tissue; i.e., what is the resolution in the third dimension? The other has to do with the efficiency of the freeze trapping procedure; i.e., how deep in the tissue is the redox state preserved at the In Vivo level? The first problem was tested on a sandwich of oxidized and reduced samples of frozen pigeon heart mitochondria. The sandwich was ground with intermittent readings of the FP and PN signals, and the thickness of the mitochondrial layer, at which the signal from the reduced/oxidized sample significantly changed the signal of the oxidized/reduced layer below, was monitored. The experiments show that mitochondria at a distance of 120 μ or more from the surface being scanned do not contribute to the FP and PN signals, but failed for technical reasons to show exactly at what distance the contribution becomes significant.

The progression of the freezing front into the tissue employing the Wollenberger freeze-clamping procedure (15) approximately follows the equation $t = x^2k$ (15,8) where t is the time requirement for the temperature in the tissue in a given distance, x , from the cooled surface to decrease, for example from 37 $^{\circ}$ C. to -20 $^{\circ}$ C. k is a constant, determined to 0.8-1.0 in muscle tissue for the temperature interval mentioned (15,1); a value of 1.4 has been measured in rat brain with the present freeze clamping setup; i.e., the first mm of tissue will be cooled from 37 $^{\circ}$ C to -20 $^{\circ}$ C within 1.0 seconds (it is assumed that the final thickness of the freeze clamped tissue block is more than 2 mm). In experiments previously described (11) where brain tissue was freeze clamped with the Guillotine-freeze clamping technique, the rapidity of the freeze trapping was evaluated by measuring the redox ratio in various depths from the cooled sample surface. The FP/PN ratio was measured in about 100 points covering the brain cross-section (cf. Fig. 9A). 320 μ of tissue was ground away from the sample at 77 $^{\circ}$ K and another series of redox ratio measurements was performed, etc. The average redox ratio measurements were calculated for each cross-section. The results showed no FP/PN decrease in the second and the third cross sections (320 and

640 μ depth) as compared to the first (0 μ depth); whereas a 40% decrease was observed in the fourth cross-section in a depth of 960 μ . Figure 10 shows a similar experiment with a normoxic brain where the redox ratio was measured on 14 consecutive cross-sections in the same sample between 0.05 and 3.9 mm of depth. Figure 10A gives the average FP/PN ratio of the brain part of the cross-section as a function of the distance from the cooled surface. The average ratio remains constant for 4 consecutive sections (between 0.05 and 0.5 mm). There is a rapid phase of reduction between 0.6 and 2.4 mm, and then a slow phase which is apparently not quite completed is a tissue depth of 3.9 mm. This shape of the progression curve suggests that the initial plateau value of FP/PN represents the In Vivo level. Assuming a k-value of 1.0 in the equation stated before, the first mm of tissues will be frozen in 1 second, the second mm in 4 seconds, etc. So by squaring the values on the x-axis in Fig. 10A, a rough estimate of the time for tissue reduction as a function of the time of ischemia (sampling-time + freezing time) may be obtained. Freezing time was defined above. Sampling time is defined as the interval between interruption of the blood-supply to the brain and the onset of freezing. Thus it can be calculated that less than a second of circulatory arrest is allowed in the normoxic brain before the redox state of mitochondria in critical locations are effected. Half reduction was reached in a distance of 1.3 mm - corresponding to about 3 seconds of ischemia. In a suspension of isolated mitochondria FP/PN will be half reduced at an oxygen concentration of about $10^{-7}M$ (6). In Fig. 10B the FP/PN ratio in four separate regions are shown. The region depicted by each of the four graphs is indicated on Fig. 9B with the same symbol. The FP/PN ratio on the left hemisphere mesencephalic region (O) and the right hemisphere cerebral cortex (●) seem to pass through a maximum at 0.5 and 0.15 mm of tissue depth respectively. The metabolic heterogeneity is obvious between 0 and 0.9 mm, but from there on all four regions largely follow the same progression curve to lower FP/PN values - after 2.3 mm the curves are almost coincident. Other regions of the cross-section have been investigated as the four regions depicted, however all seem to follow the pattern described above.

In case the oxygen consumption rate in one region was greater than in another and the oxygen availability the same at the time of sampling, one would expect a shorter plateau phase as well as a steeper slope for the high oxygen consumption area. A difference in oxygen availability in two regions with the same oxygen consumption rate would also result in a shorter plateau phase but the slope should not change. The progression curve for the right hemisphere mesencephalic region (Δ) might represent an area with low oxygen availability as the decrease of FP/PN starts already after 0.15 mm, however the rest of the progression curve does not seem left displaced.

All in all we conclude that there is no major regional imbalance between oxygen consumption and oxygen availability in normoxic rat brain.

REFERENCES

1. Cain, D.F., R.E. Davis (1964). Rapid Mixing and Sampling Techniques in Biochemistry, p. 229. Academic Press, New York.
2. Chance, B., A. Azzi, I.Y. Lee, C.P. Lee, and L. Mela (1969). FEBS Symposium, VOL: 17, p. 233.
3. Chance, B., N. Oshino, T. Sugano, A. Mayevsky. (1973). Oxygen Transport to Tissue, p. 227.
4. Chance, B., N. Graham, V. Legallais. (1975). Anal. Biochem. VOL:67 p. 552.
5. Chance, B., V. Legallais, J. Sorge, N. Graham. (1975). Anal. Biochem. VOL:66, p. 498.
6. Sugano, T., N. Oshino, B. Chance. (1974). Biochem. et Biophys. Acta VOL:347, p. 340.
7. Chance, B., R. Oshino. In preparation.
8. Hendrix, B.C. Handbook of Chemistry and Physics. p. F75. Chemical Rubber Co., Cleveland, Ohio.
9. Ji, S., B. Chance, B.H. Stuart, R. Nathan. Brain Research. In Press.
10. Nordberg, K., B. Quistorff, B.K.Siesjö. (1975). Acta Physiol. Scand. VOL:95, p. 301.
11. Quistorff, B., S. Eleff, R. Oshino, B. Chance. Proceedings of the 10th FEBS Meeting. In Press.
12. Quistorff, B., B. Chance. Analytical Biochemistry. In Preparation.
13. Quistorff, B. (1975). Anal. Biochem. VOL:68, p. 102.
14. Smith, T., S. Ji. In Preparation.
15. Wollenberger, A., O. Ristau, G. Schoffa. (1960). Pflügers Arch. VOL:270, p. 399.

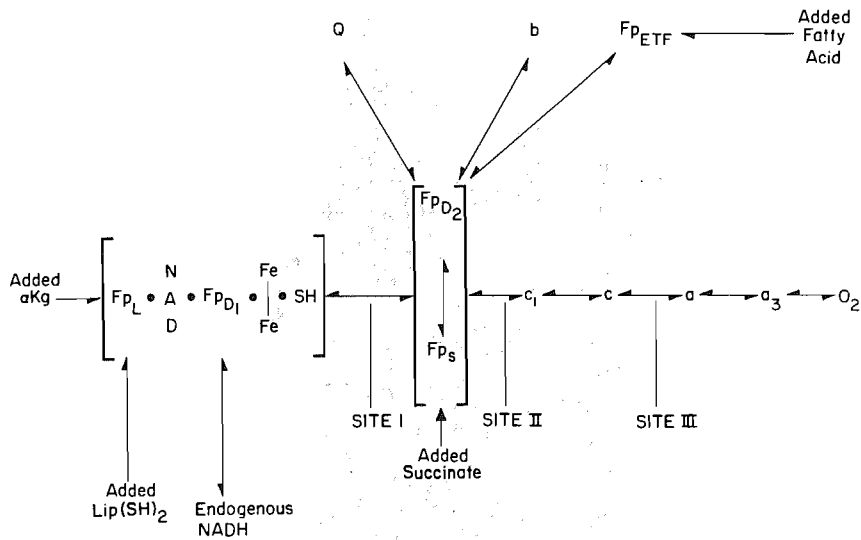
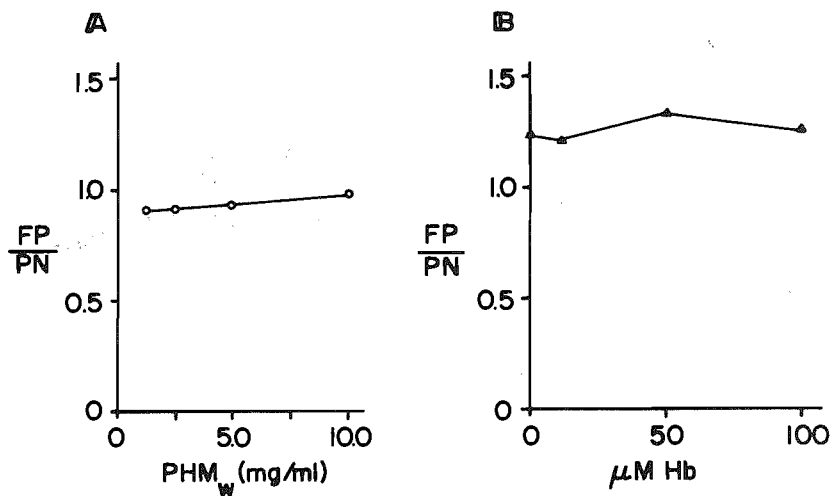


Figure 1. Schematic diagram of the components of the respiratory chain of rat liver mitochondria. Taken from Chance *et al.* 69 (2).



RO100-107B

Figure 2. Effect of changes in mitochondrial- and hemoglobin concentration of FP/PN ratio. Measurements were made on pigeon heart mitochondria at 80°C. Taken from Chance *et al.* (76) (7).

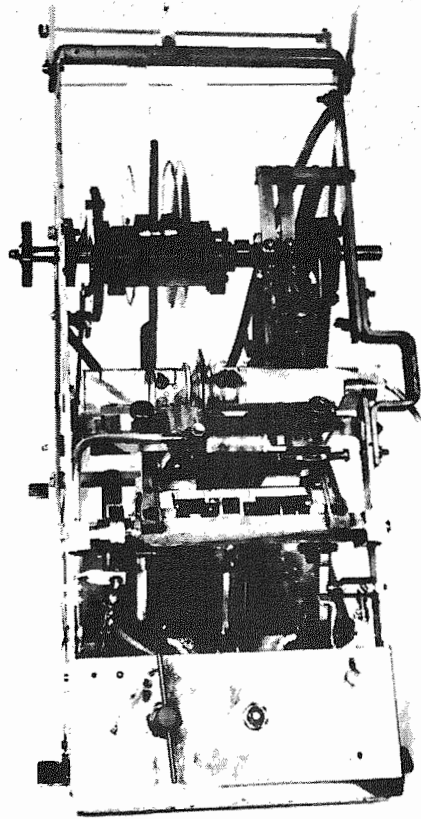


Figure 3. The Guillotine-freezeclamping instrument.

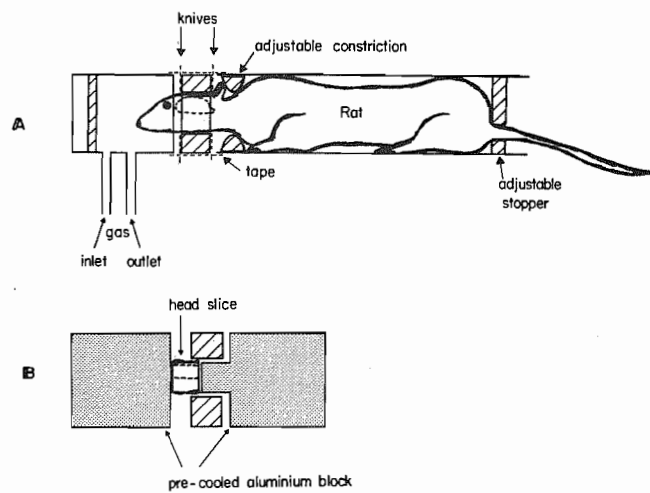


Figure 4. The principle of the Guillotine-freezeclamping procedure.
 A. The rat is restrained in the tube of the instrument and a cross section between the two vertical dotted lines is cut out.
 B. The liberated head slice is freezeclamped.

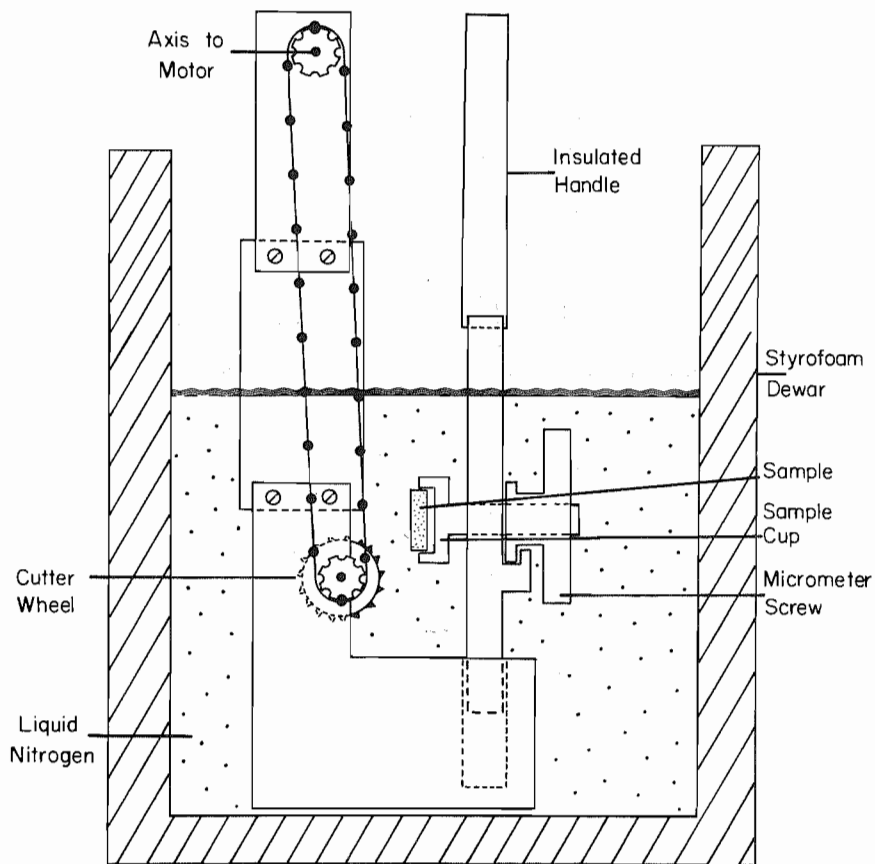
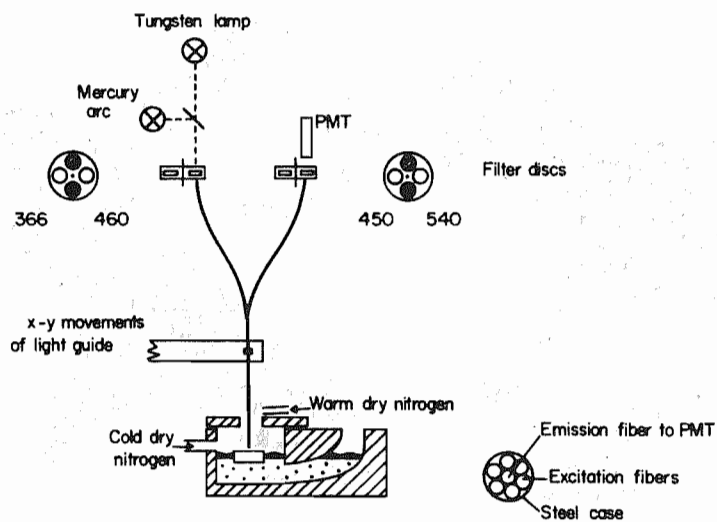
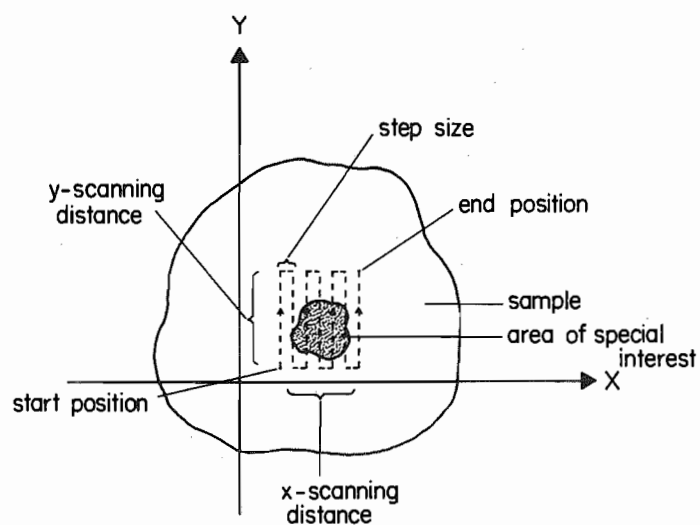


Figure 5. The low temperature tissue miller.



BQ 74

Figure 6. The light guide scanner. Two of the four channels of the fluorometer are used with the filter configuration shown. The part of the light guides from the fluorometer to the merging point are flexible and allows for the scanning movements of the lower rigid part connected to the x-y cross ways. The configuration of the fibers in the merged part of the light guide is shown in the lower right hand corner of the figure.



BQ 83

Figure 7. Diagram of the scanning pattern.

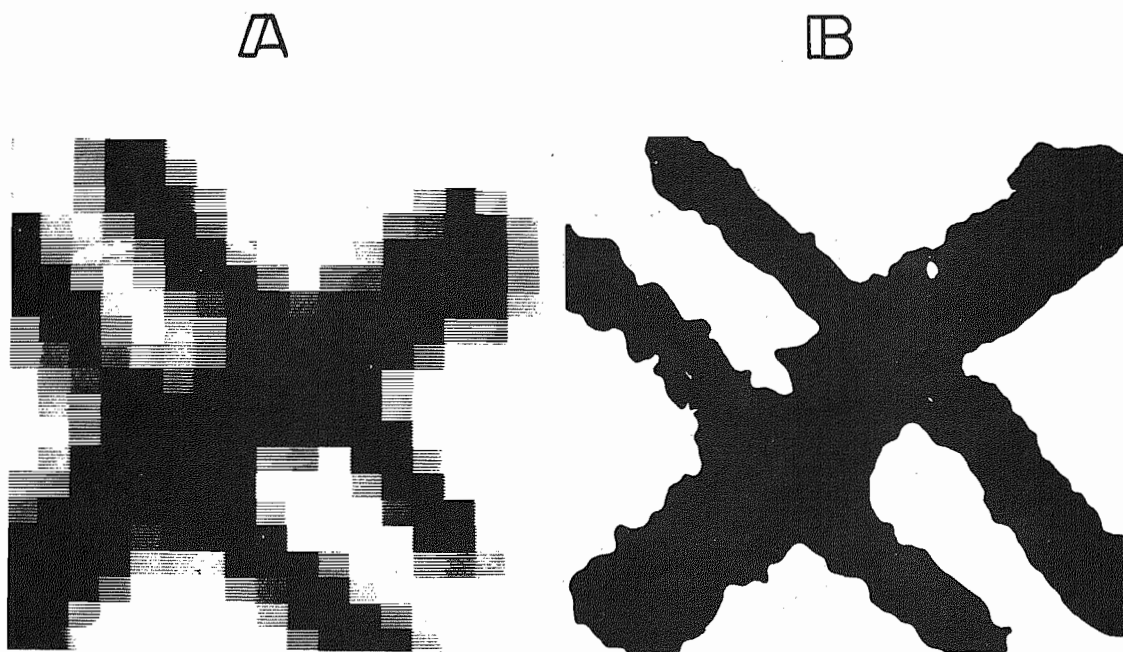


Figure 8. A. Reconstructed 'PN image' of a test pattern, scanned with the light guide fluorometer shown in Figure 6. B. Photo of the same test pattern.

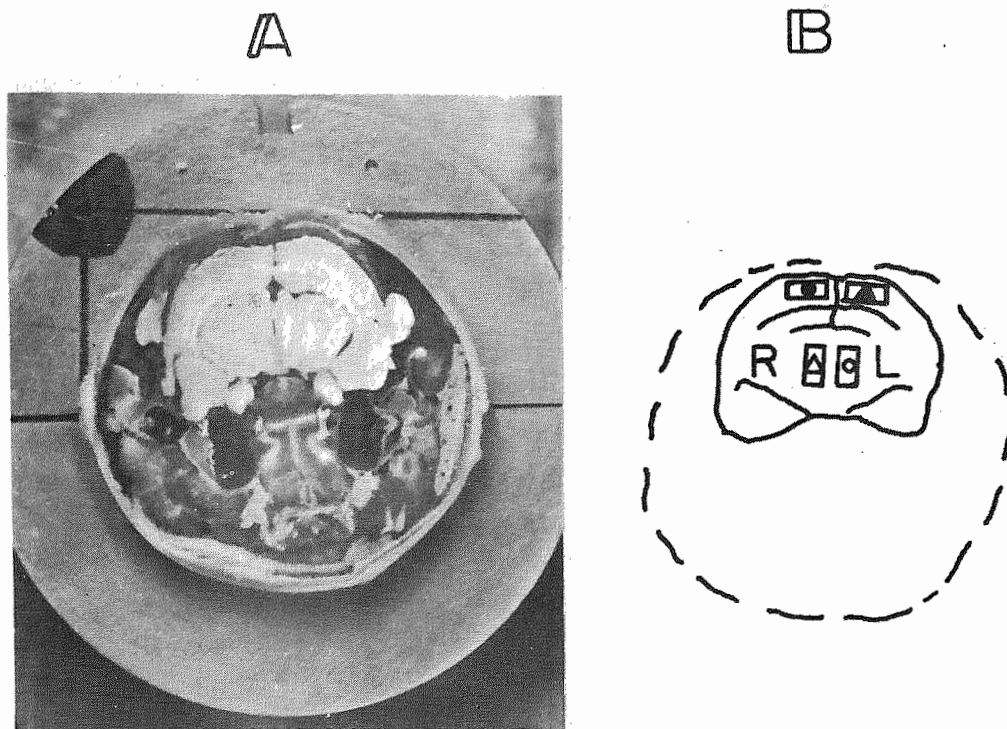


Figure 9: A. The freezeclamped cross-section of the rat head mounted in the sampleholder of the tissue miller (cf. Fig. 5). The picture was taken with the sampleholder partially submerged in liquid nitrogen. The surface depicted was the "2.4 mm surface" from the experiment shown in Fig. 10.
 B. Shows the brain cross section schematically. The rectangles indicate the subregions from where the measurements given in Fig. 10B were made.

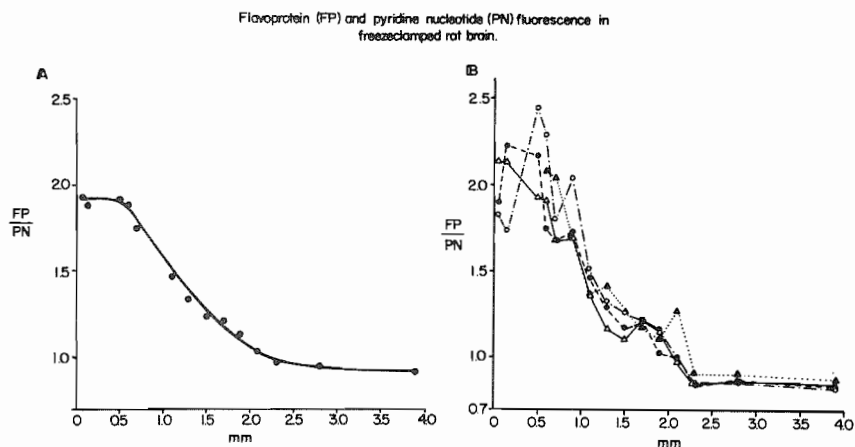


Figure 10. The brain was freezeclamped with the Guillotine-freezeclamping technique from a pentobarbital anaesthetized male Wistar rat weighing 205 grams. The "0 mm cut" corresponding to the left of the vertical dotted lines on Figure 3A, was made at a distance of 6 mm from the posterior end of the cerebral cortex. The fluorometer was calibrated on a fluorescent paper standard which gives a FP/PN ratio of 7.3 on oxidized pigeon brain mitochondria. The aperture of the instrument was 0.7 mm and about 120 readings were made from the brain part of each cross section

A. Gives the relation between the average FP/PN ratio of the cross section and the distance from the cooled surface.

B. Shows the FP/PN ratio in symmetrical regions of the two hemispheres. The location of the 4 regions on the brain cross section is given in Figure 9B. The same regions were picked in each of the 14 cross sections, so the graphs are 2-D representations of 4 separate tissue columns. Each region is about 7 mm² and the average value of 6-9 FP/PN measurements within the region are given. There were no measurements of the cortical region in the left hemisphere in the first three scans (0.05, 0.15 and 0.5mm).